Shape Filtering for False Positive Reduction at Computed Tomography Colonography

Abhilash A. Miranda*, Tarik A. Chowdhury, Ovidiu Ghita,
and Paul F. Whelan

Vision Systems Group, Dublin City University, Ireland
abhilash@eeng.dcu.ie

Abstract. In this paper, we treat the problem of reducing the false positives (FP) in the automatic detection of colorectal polyps at Computer Aided Detection in Computed Tomography Colonography (CAD-CTC) as a shape-filtering task. From the extracted candidate surface, we obtain a reliable shape distribution function and analyse it in the Fourier domain and use the resulting spectral data to classify the candidate surface as belonging to a polyp or a non-polyp class. The developed shape filtering scheme is computationally efficient (takes approximately 2 seconds per dataset to detect the polyps from the colonic surface) and offers robust polyp detection with an overall false positive rate of 5.44 per dataset at a sensitivity of 100% for polyps greater than 10mm when it was applied to standard and low dose CT data.

1 Introduction

According to the World Health Report [1], colorectal cancer caused approximately 622,000 deaths in 2002. It is understood that the risk of colon cancer could be reduced considerably if growths in the colon called polyps are removed before they become cancerous.

CAD-CTC is being developed as a reliable technique for early detection of premalignant polyps useful in mass screening of risky individuals. It involves the analysis of the images of the colon obtained using a Computed Tomography (CT) examination of the abdominal region. Computer vision is used for the automatic detection of potential polyps by analyzing the three-dimensional model of the colon obtained by combining the two-dimensional axial images obtained from the CT examination. Many methods developed for CAD-CTC suffer from severe false-positive (FP) findings owing to the confusion in correctly distinguishing polyps from other colonic shapes such as folds, residual materials, etc.

In this paper, we propose a novel method to accurately discriminate the polyp shapes from other colonic shapes (folds) by analysing a reliable shape distribution function (SDF) in the frequency domain. After a detailed analysis of the SDF in the frequency domain, we developed a novel technique that addresses the polyp−non-polyp classification as a shape filtering problem. In order to evaluate

---

* Corresponding author.

the validity of the proposed technique we have analysed its performance when applied to a large number of synthetic (scanned with standard and low radiation dose) and real CT datasets (scanned at a standard radiation dose).

This paper is organised as follows. In section 3, the method designed to extract the candidate surfaces from the CT data is briefly explained. In section 4, we introduce the SDF of an extracted colonic surface and discuss its properties. The next two sections discuss the properties of the polyp and non-polyp SDFs and explain the motivation for analysing the SDF in the frequency domain in terms of its power spectral density. In section 5.1, we detail the implementation of the novel shape filtering scheme developed for polyp−non-polyp classification. In the concluding section, we present the results obtained on the large number of real patient datasets on which the shape filtering technique was tested.

2   Materials and Method

In order to perform bowel cleansing, the patients were instructed to follow a low-residue diet for 48 hours, followed by the ingestion of clear fluids for 24 hours. Before the examination, the colon is gently insufflated with room air at the maximum level tolerated by the patient and the CT data acquisition was performed on a Siemens-Somatom 4-slice multi-detector spiral CT scanner by the radiologists at the Mater Hospital, Dublin, Ireland. The scanning parameters in use are 120kVp, 100mAs tube current, 2.5mm collimation, 3mm slice thickness, 1.5mm reconstruction interval, and 0.5 gantry rotation. The scanning is performed in a single breath-hold and the acquisition time is in the interval of 20 to 30 seconds depending on the body-size of the patient. The scanning is performed first with the patient in the supine position and then repeated with the patient in the prone position. Typically the number of slices varies from 200 to 350 and the total size of the volumetric CT data is approximately 150MB.

3   Candidate Surface Extraction

The candidate surface extraction method consists of two main stages. In the first stage, the colonic wall is identified in the CT data based on the high contrast between the gas insufflated regions and the colon tissue. In this way, the gaseous region can be successfully identified by using a simple region growing algorithm where the colonic wall is defined by the voxels that are adjacent to the colon tissue. The threshold value for region growing algorithm was set to $-800\,$HU [2] to ensure that only the voxels inside the colon (gas filled volume) are segmented. The second stage of the algorithm attempts to identify the convex surfaces from the colon wall by analysing the intersections of the normal vectors which are calculated using the Zucker-Hummel operator [3]. The normal intersections are recorded for a number of Hough points that are uniformly distributed from 2.5 mm to 10 mm in the normal direction for each voxel of the colon wall. The normal intersections are recorded into a 3D histogram and the candidate surfaces are generated by the Hough points that have more than 5 intersections in the 3D histogram. In order to

eliminate the voxels associated with spurious non-convex surfaces an additional convexity test is performed [2],[4]. During the candidate surface processing, the centre-point and the radius of each candidate cluster is calculated by finding the sum of weighted Gaussian distances d_G for each point of the surface (full details about the implementation of this algorithm can be found in [2]).

4   Shape Distribution Function

Robust polyp detection is very difficult to achieve since the polyps and other convex colonic structures such as folds have a large number of shapes and sizes. Typically the polyps can be assumed to have a spherical shape where the nominal model for folds is cylindrical. Based on this geometrical characterization, many researchers attempted to perform the polyp/fold classification using geometrical features that are extracted from candidate surfaces [5][6][7]. Unfortunately very often the polyp and fold surfaces present very subtle shape differences as illustrated in Fig. 1 and as a result the geometrical approaches return high sensitivity in polyp detection but at the expense of an increased number of false positives.
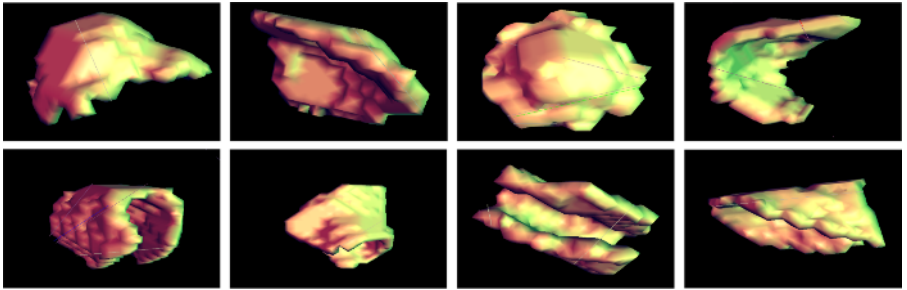
Fig. 1. Images illustrating some examples of the extracted surfaces for polyps (first row) and folds (second row)

In the next section we detail the shape distribution function and describe its properties that make it suitable for robust polyp−non-polyp classification.

4.1   Definition and Properties

For a given candidate colonic surface, the computation of the shape distribution function that we use in this paper can be explained as follows. Given the coordinates of the n voxels defining the candidate surface **U** and the Gaussian center **v** of the voxels [4] associated with the candidate surface, we find the $n-$length array **w** which lists the Euclidean distances between each of the n surface voxels and the Gaussian center **v** of the candidate surface **U**. We call the histogram **x** of the entries in **w** as the shape distribution function(SDF) of the candidate colonic surface **U**, which is a *distribution function* of the relative distances of the surface voxels of the candidate colonic surface.

The SDF **x** is simple in definition and computationally efficient. Also, **x** is robust to characterise the shape of the candidate surface when the voxel data is sparse or affected by noise. Since **x** is invariant to rotation and translation of the surface, it has a very important advantage that it is dependent only on the colonic shape and independent of the colonic orientation. The SDF used here is similar to the shape distribution function *D1* used for object recognition [8].

Another important benefit in using the SDF is the significant reduction in the dimensionality that is achieved by transforming 3D data (**U**) to a 1D time-series (**x**) without losing interesting shape cues. This dimensionality reduction, as discussed later, reduces the complexity of the analysis thus making it suitable for real-time operation.

5   Analysis of the SDFs Using the Autocorrelation Functions

Some of the observed general characteristics and behaviours of the 3−neighbour averaged samples SDFs of polyps and non-polyps illustrated in Fig. 2 are as follows. The SDF of a polyp is, in general, a smooth curve having a single and global maxima. Conversely, a non-polyp SDF is noisy and might have single or multiple maxima, which might be similar to that of polyps, but whose location or variance near the neighbourhood of the maxima are random.
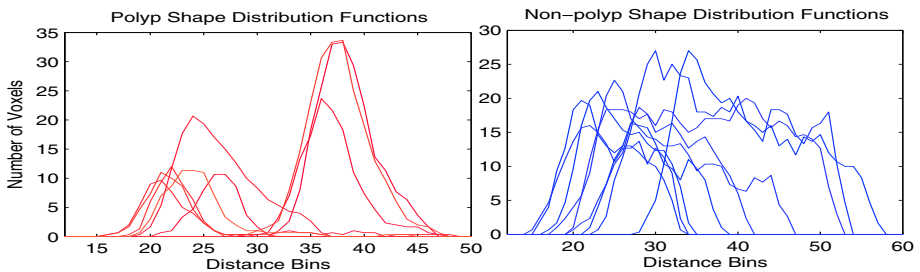
Fig. 2. SDFs of polyps and non-polyps surfaces from real-datasets shows significant differences in smoothness and maxima characteristics

We now briefly describe the observed characteristics of the SDF and evaluate the need to analyse the autocorrelation functions of the SDF for obtaining the information that differentiates the polyp surfaces from non-polyp surfaces.

Although the SDFs for polyp and fold surfaces depicted in Fig. 2 offer the primary discrimination between these surfaces, there is no robust directly recognisable shape for the SDF curve for any one of the classes. As a result, we cannot apply straight-forward SDF shape matching technique to classify polyps from non-polyps. In addition, since there are multiple maxima with unpredictable variances in their neighbourhoods for a non-polyp SDF, techniques based on probability density function fitting or variance-based feature extraction will be less efficient in finding optimal patterns to classify non-polyp surfaces correctly.

Since the polyp and non-polyp SDFs are generated by unknown probability distributions and appear to be corrupted by noise, there is an uncertainty in the location and variance of the maxima in the SDFs. Hence, it is necessary to compare each of the SDF time-series **x** with a delayed version of itself and others. This can be done by analysing the autocorrelation functions R_{xx} of the SDFs.

Moreover, in order to study the effects of noisy frequency components on the variance (power) of the SDF, it is necessary to see the contribution of the various frequency components of **x** to the total variance. According to the Wiener-Khinchin theorem, the power spectral density S_{xx} of a signal **x** is the Fourier transform of R_{xx}. In practice, for computational purposes, the S_{xx} is calculated using Fast Fourier Transform methods.

5.1   Power Spectral Density of SDFs

order to understand the distribution of the variance of the SDFs in the frequency domain, we analyse the power spectral density of the SDFs on which we make certain interesting observations which help us to design a robust shape filtering scheme as explained in this section.

Let $\mathbf{x} = x_0, \ldots, x_{M-1}$ be the time-series corresponding to an SDF. The samples of its discrete Fourier transform is given by $X_l = \sum_{k=0}^{M-1} x_k e^{\frac{-i2\pi kl}{M}}$ so that the power spectral density of SDF is given by $S_{xx_l} = X_l X_l^*$, the product of X_l and its conjugate and normalised in accordance with the desired resolution of X_l.

We used a 128-point FFT to compute the power spectral density S_{xx} of the SDFs and we noticed that S_{xx} of the fold surfaces attenuate much quicker than those associated with polyps. Our experiments indicate that the frequency f_{dB} at which S_{xx} reaches 12.5% of its power at DC frequency offers a robust discrimination between the polyp and fold surfaces as illustrated in the Fig. 3.
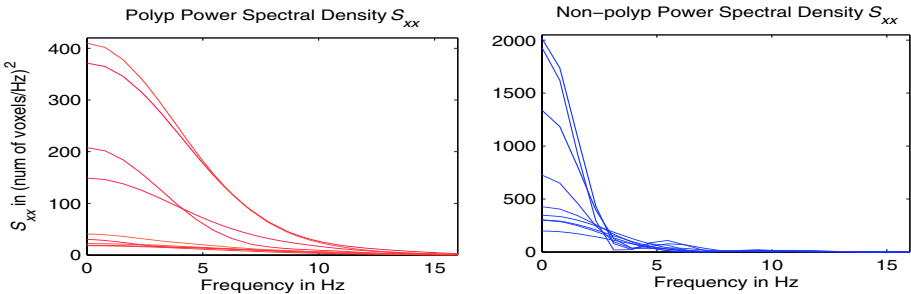
Fig. 3. S_{xx} for the Shape Distribution Functions used in Fig.2 shows faster attenuation for Non-polyps than Polyps

Thus the classification criterion can be defined as follows: an SDF belongs to the polyp class if its f_{dB} is higher than an experimentally selected threshold frequency f_{th}.

The threshold-based rejection rule mentioned above works very well for small and medium sized polyps but it rejects very large polyps whose SDFs are not

very different from those associated with folds. Based on observations on an experimental set of samples, we find that for certain large polyps f_{dB} lies in an uncertain classification region $f_{min} < f_{th} < f_{max}$. References [4] and [2] have shown that the sum of the weighted Gaussian distances d_G of the voxels that define the candidate surface offers robust discrimination between the surfaces associated with large polyps and those derived from folds. Based on the experimentation with various sizes of polyps having a weighted sum of Gaussian distances, d_1 and d_2, corresponding to f_{min} and f_{max}, we devised a technique to compute adaptively the classification threshold frequency f'_{th} according to the following linear function: $f'_{th} = f_{max} + (d_G - d_2) \frac{f_{min} - f_{max}}{d_1 - d_2}$. In this way, a SDF belongs to a polyp surface if its f_{dB} is higher than the computed threshold frequency f'_{th}, otherwise it is classed as a fold surface.

6   Experiments and Results

In this section we discuss the tests that we carried out using the shape filtering scheme and present the results obtained which we compare with other established CAD-CTC techniques.

The shape filtering CAD-CTC technique was tested on 61 real datasets obtained as part of the clinical study in conjunction with the Mater Hospital, Dublin, Ireland. The shape filtering technique was also tested on custom-built phantom datasets [9] which contain a large number of synthetic structures which replicate accurately the real polyp shapes encountered in clinical studies.

One of the main concerns associated with CTC as a mass screening technique for colorectal polyp detection is the patient exposure to ionising radiation. A reduction in the radiation dose will increase the level of noise in the CT data and our aim is to fully evaluate the impact of the radiation dose on the performance of our CAD-CTC system. In this regard, we have used in our experiments a synthetic phantom that have 47 synthetic polyps that have different shapes (sessile, pedunculated and flat) and sizes (3 to 18mm). In our experiments we used the phantom CT data that has been obtained for the following radiation doses: 100mAs, 60 mAs, 20mAs, and 13mAs. The results of the shape filtering CAD-CTC for the Phantom Data [9] are summarised in Tables 1 to 4. The experimental results indicate that the radiation dose does not have a significant impact on the performance of our polyp detection method since the sensitivity for clinical relevant polyps (larger than 10mm) is not affected. A small reduction in sensitivity for polyps in the range 5-10mm has been noticed when the data has been scanned with 20mAs radiation dose.

Table 5 shows the performance of the shape filtering technique when applied to 61 real patient datasets. These results were validated by our clinical partners from the Mater Hospital, Dublin, Ireland and indicate that the technique achieved 100% sensitivity for detection of polyps larger than >10mm which are the most important features to be examined in clinical studies. The experimental data also show that there is a high true positive rate for polyps with sizes ranging between 5mm - 10mm where a sensitivity of 81.25% is achieved in spite of some polyps

Table 1. Phantom Data (100 mAs)

Polyp Type	Total Polyps	True Positives	Sensitivity %
≥ 10 mm	14	14	100
[5, 10) mm	19	19	100
< 5 mm	5	4	80
Flat	9	2	22.22
Total	47	39	83.97

Phantom Dataset(100 mAs): FP = 1

Table 2. Phantom Data (60 mAs)

Polyp Type	Total Polyps	True Positives	Sensitivity %
≥ 10 mm	14	14	100
[5, 10) mm	19	19	100
< 5 mm	5	4	80
Flat	9	3	33.33
Total	47	40	85.11

Phantom Dataset(60 mAs): FP = 1

Table 3. Phantom Data (20 mAs)

Polyp Type	Total Polyps	True Positives	Sensitivity %
≥ 10 mm	14	14	100
[5, 10) mm	19	17	89.47
< 5 mm	5	3	60
Flat	9	2	22.22
Total	47	36	76.60

Phantom Dataset(20 mAs): FP = 0

Table 4. Phantom Data (13 mAs)

Polyp Type	Total Polyps	True Positives	Sensitivity %
≥ 10 mm	14	12	85.71
[5, 10) mm	19	18	94.74
< 5 mm	5	3	60
Flat	9	1	11.11
Total	47	34	72.34

Phantom Dataset(13 mAs): FP = 1

Table 5. Real Datasets (100 mAs)

Polyp Type	Total Polyps	True Positives	Sensitivity %
≥ 10 mm	10	10	100
[5, 10) mm	32	26	81.25
< 5 mm	104	62	59.62
Mass	11	7	63.64
Flat	2	1	50
Total	159	106	66.89

FP/ Real Dataset = 5.44

having very complex shapes. The false positives returned by our shape filtering method stands at an average of 5.44 per dataset and compares well with the techniques that will be examined in the next section.

The method detailed in this paper has not been developed to primarily detect the flat polyps since these polyps have many geometrical characteristics that are similar with those of the folds. High sensitivity for flat polyps detection cannot be achieved by using methods that attempt to discriminate the polyp and fold surfaces based on global shape models and the flat polyps should be approached as a distinct category of polyps.

The average time for surface extraction per dataset for processing each volume of data is approximately 80 seconds on a Pentium-IV 3-GHz processor machine with 1GB memory. The computation of the power spectral density S_{xx} and the shape-filtering process takes in average 2 seconds per dataset when the algorithm was executed on the same machine.

6.1   Comparison with Established Techniques

In order to evaluate the validity of our shape filtering CAD-CTC we compare its performance with the results in polyp detection obtained by other relevant

documented techniques. Though they were not tested on the same datasets, the reported sensitivity and false positive per dataset (FP) should be indicative of their relative robustness in polyp detection.

For polyps larger than 10mm, the CAD-CTC techniques evaluated in this section present the following results. The method developed by Summers et al. [5] which uses surface curvature information gives a sensitivity of $29\% - 100\%$ with a varying FP rate $(6 - 20)$ depending on the scanning parameters. The method proposed by Vining et al. [6] based on surface extraction and curvature analysis recorded a 73% sensitivity with a very inconsistent FP rate in the range $9 - 90$. Yoshida et al. [7] used various shape indices (cup, rut, saddle, ridge, cap) and curvedness values on small volumes of interest in conjunction with fuzzy clustering. They report a sensitivity of 89% with an FP of 2.0 which increased by a factor of 1.5 when sensitivity was increased to 100%.

For polyps larger than 5mm, the technique developed by Kiss et al. [4] based on surface normal distribution and sphere fitting achieves a sensitivity of 90% with a FP of 2.82. It is useful to note that this performance is obtained when they applied their method to high resolution CT data (0.8mm reconstruction interval). We have evaluated the performance of our shape filtering technique on CT data with a lower resolution (1.5mm reconstruction interval) where the problems caused by the partial volume effects are more pronounced.

The SDF based shape filtering technique that we presented in this paper, achieved 100% sensitivity for polyps greater than 10mm and 81.25% sensitivity for polyp sizes between $5 - 10$mm with an overall FP of 5.44. The performance in polyp detection of our polyp detection technique compares well with the performance returned by the CAD-CTC systems evaluated in this section.

7   Conclusion

We have designed and implemented a simple, stable and robust CAD-CTC technique which attains better results than other published CAD-CTC techniques. Currently, the false positive rate stands at an average of 5.44 FPs per dataset that can be further reduced by fine tuning the technique to increase the detection rate for flat polyps. For this category of polyps, the developed shape filtering technique achieved the lowest sensitivity. By taking the 3D shape recognition into the Fourier domain analysis, we were able to simplify the problem with significant reductions in processing time. We envisage further extensions to the shape-distribution based shape recognition technique to further improve the performance in polyp detection for small and medium polyps.

Acknowledgments

References

1. World Health Organisation: The World Health Report 2004. WHO (2004)
2. Chowdhury, T., Ghita, O., Whelan, P.: A Statistical approach for Robust Polyp Detection in CT Colonography. Proceedings of the International Conference of the IEEE Engineering in Medicine and Biology Society **27** (2005)
3. Zucker, S.W., Hummel, R.A.: A Three-Dimensional Edge Operator. IEEE Transactions on Pattern Analysis and Machine Intelligence **3** (1981) 324–331
4. Kiss, G., Cleynenbreugel, J., Thomeer, M., Suetens, P., Marchal, G.: Computer Aided Diagnosis for Virtual Colonography. MICCAI (2001) 621–628
5. Summers, R., Johnson, C., Pusanik, L., Malley, J., Youssef, A., Reed, J.: Automated Polyp Detection at CT Colonography: Feasibility Assessment in a Human Population. Radiology **216** (2000) 284–290
6. Vining, D., Hunt, G., Ahn, D., Steltes, D., Helmer, P.: Computer-Assisted Detection of Colon Polyps and Masses. Radiology **219** (2001) 51–59
7. Yoshida, H., Masutani, Y., MacEneaney, P., Rubin, D., Dachman, A.: Computerized Detection of Colonic Polyps at CT Colonography on the Basis of Volumetric Features: Pilot Study. Radiology **222** (2002) 327–336
8. Osada, R., Funkhouser, T., Dobkin, D.: Matching 3D Models with Shape Distributions. International Conference on Shape Modeling and Applications (2001) 154–166
9. Chowdhury, T., Sadleir, R., Whelan, P., Moss, A., Varden, J., Short, M., Fenlon, H., MacMathuna, P.: The Impact of Radiation Dose on Imaged Polyp Characteristics at CT Colonography: Experiments with a Synthetic Phantom. Technical report, Association of Physical Scientists in Medicine, Annual Scientific Meeting, Dublin (2004)